Correlation among maximum standardized ^{18}F-FDG uptake and pathological differentiation, tumor size, and Ki67 in patients with moderately and poorly differentiated intrahepatic cholangiocarcinoma

Yiqiu Zhang[1,2,3,4] **MD,**
Beilei Li[1,2,3,4] **MD, PhD**
Yibo He[1,3,4] **MD,**
Lifang Pang[1,3,4] **MD,**
Haojun Yu[1,3,4] **MD,**
Hongcheng Shi[1,2,3,4] **MD, PhD**

**Yiqiu Zhang and Beilei Li equally contributed to this work*

1. Department of Nuclear Medicine, Zhongshan Hospital, Fudan University, Shanghai, 200032, China
2. Department of Nuclear Medicine, Xiamen Branch, Zhongshan Hospital, Fudan University, Fujian, 361015, China
3. Nuclear Medicine Institute of Fudan University, Shanghai, 200032, China
4. Shanghai Institute of Medical Imaging, Shanghai, 200032, China

Keywords: PET/ CT -^{18}F-FDG - Intrahepatic cholangiocarcinoma

Corresponding author:
Hongcheng Shi MD, PhD,
Department of Nuclear Medicine, Zhongshan Hospital, Fudan University,
Nuclear Medicine Institute of Fudan University,
Shanghai Institute of Medical Imaging, Shanghai, 200032, China.
Phone: 00862164041990-2064
shihongcheng163@163.com

Received:
10 October 2021
Accepted revised:
15 March 2022

Abstract

Objective: To investigate the correlation among the maximum standardized uptake value (SUVmax) on fluorine-18-fluorodeoxyglucose (^{18}F-FDG) positron emission tomography/computed tomography (PET/CT) and tumor differentiation, size, and Ki67 in patients with moderately and poorly differentiated intrahepatic cholangiocarcinoma (ICC). **Materials and Methods:** The ^{18}F-FDG PET/CT imaging data of 116 patients with single ICC lesions confirmed by pathology were retrospectively evaluated. Pathological characteristics of the tumor such as the largest tumor diameter, differentiation, Ki67 expression, SUVmax of the primary tumor, and the tumor to normal background ratio (TNR) were recorded. **Results:** Among the 116 lesions, 45, 51, and 20 lesions were classified into the moderately differentiated, moderately-poorly, and poorly differentiated groups, respectively. There were significant differences in the SUVmax (P=0.033) and TNR (P=0.044) among the three groups. Maximum SUV was significantly correlated with differentiation (r=0.244, P=0.008). When the cases were categorized according to the tumor size (group 1, ≤3cm, n=14; group 2, >3 and ≤5cm, n=37; group 3, >5 and ≤10cm, n=52; group 4, >10cm, n=13), there were significant differences in the SUVmax (P< 0.001) and TNR (P<0.001) among the four groups. Maximum SUV was significantly correlated with tumor size (r=0.481, P<0.001). Among the 116 lesions, 38 lesions and 78 lesions were classified into the low Ki67 and high Ki67 expression groups, respectively. There were significant differences in the SUVmax (P=0.028) and TNR (P= 0.007) between the two groups. Maximum SUV was significantly correlated with Ki67 expression (r=0.242, P= 0.009). **Conclusion:** In moderately and poorly differentiated ICC, the SUVmax and TNR are significantly associated with tumor differentiation, size, and Ki67 expression.

Hell J Nucl Med 2022; 25(1): 38-42 *Epub ahead of print: 8 April 2022* *Published online: 29 April 2022*

Introduction

Intrahepatic cholangiocarcinoma (ICC) is the second most common primary hepatic malignancy after hepatocellular carcinoma (HCC), accounting for about 5%–30% of primary hepatic cancers [1]. Fluorine-18-fluorodeoxyglucose (^{18}F-FDG) positron emission tomography/computed tomography (PET/CT) has obvious advantages in the diagnosis, staging, re-staging, and prognosis evaluation of ICC [2-7]. For tumor diagnosis, ^{18}F-FDG PET/CT is based on the degree of ^{18}F-FDG uptake and the degree of ^{18}F-FDG uptake in ICC lesions has a certain relationship with tumor size and differentiation [8]. The degree of tumor differentiation is negatively correlated with the degree of malignancy. Ki67, as a marker of tumor cell proliferation activity, often reflects the number of tumor cell proliferation and demonstrates the malignancy of the tumor. The purpose of this study was to investigate the correlation among the maximum standardized uptake value (SUVmax) of ^{18}F-FDG PET/CT imaging of low and moderately differentiated ICC and tumor size, degree of pathological differentiation, and Ki67 expression.

Materials and Methods

Patients

All patients included in this study were suspected of having a space-occupying lesion in the liver and were those in which the first preoperative PET/CT examination was performed for diagnosis and staging. Patients who had not undergone further surgical resection because of a definitive diagnosis on preoperative biopsy and those who had a clear

previous history of malignancy, including a history of HCC or other malignancies were excluded. Based on the inclusion and exclusion criteria, a retrospective analysis was performed on 116 patients (60 male, 56 female; age range 29-79 years, mean age: 59.8±9.3 years) with primary ICC lesions, who underwent ^{18}F-FDG PET/CT imaging at the Department of Nuclear Medicine, Zhongshan Hospital, Fudan University.

PET/CT scan

Imaging and data acquisition was performed on a combined PET/CT system (Discovery VCT 64, GE Medical Systems, Milwaukee, WI, USA; or uMI 510, United Imaging Healthcare Co., Ltd. Shanghai, China). Patients were instructed to fast for at least 6h before the intravenous injection of 4.44MBq/kg ^{18}F-FDG. Six to eight-bed positions from the base of the skull to midthighs were imaged. For each position, the emission image was acquired for 2min. The PET images were reconstructed by using filtered back projection. Computed tomography data were acquired without IV or oral contrast agents. The CT scan data were collected with 120Kv, 140mA. All CT scans were obtained by using 3.75-mm-thick axial slices. Computed tomography data was used to attenuate PET images. CT images were reconstructed with a thickness of 1.25mm and a 512×512 matrix.

Data analysis

Positron emission tomography/CT results were analyzed and interpreted by two experienced nuclear medicine physicians. For semi-quantitative analysis, the SUVmax and tumor-to-normal liver tissue ratio (TNR) were analyzed. Maximum SUV of a normal liver was acquired and regions of interest (ROI) were drawn on the right lobe of the normal liver. Each ROI was measured as a circle with a diameter of 1.5cm.

Pathology

All patients underwent tumor resection to obtain a pathological diagnosis. The size of the lesions was measured from the pathological specimens and if there were multiple lesions, only the largest lesion per patient was selected for inclusion in this study. Tumors were divided into 4 groups (group 1: ≤3cm, group 2:>3 and ≤5cm, group 3:>5 and ≤ 10cm, and group 4:>10cm) according to the maximum diameter of tumors measured by pathological specimens. According to the degree of tumor pathological differentiation, tumors were divided into three groups (moderately differentiated, moderately-poorly differentiated, and the poorly differentiated). Ki67 expression levels were graded as shown: <10% (-), 10–25% (+), 26–50% (++), 51–70% (+++), and >75% are (++++); low expression group: (-) and (+); high expression group: (++), (+++) and (++++) group are classified as [9].

Statistical Analysis

SPSS 22.0 software for Windows (IBM Corporation, Armonk, NY, USA) was used for statistical analysis. P<0.05 indicates a significant difference. Quantitative data for the normal distribution are expressed as mean±SD, and quantitative data for skewed distribution are expressed as median and quartile range.

First, the differences of SUVmax and TNR among different groups of the tumor pathological differentiation, the tumor maximum diameter, and Ki67 expression lesions were compared. Analysis of variance was used to compare the quantitative data that satisfied normality and homogeneity of variance. The Kruskal–Wallis rank-sum test was used to compare the quantitative data that did not meet normality or homogeneity of variance.

Then, the relationship among tumor size and SUVmax, tumor differentiation and SUVmax, and Ki67 expression level and SUVmax were analyzed. Pearson's correlation analysis was used for the quantitative data of normal distribution, and Spearman correlation analysis was used for the quantitative data of skewed distribution.

Results

Among the 116 lesions, 45 lesions were classified into the moderately differentiated group, 51 lesions into the moderately-poorly differentiated group, and the remaining 20 lesions into the poorly differentiated group. There were significant differences in the SUVmax (P=0.033) and TNR (P=0 .044) among the three groups (Table 1). As tumor differentiation decreases, SUVmax and TNR gradually increase.

When the cases were categorized according to tumor size (group 1: ≤3cm, n=14; group 2:>3 and ≤5cm, n=37; group 3: >5 and ≤10cm, n=52; group 4:>10cm, n=13), there were significant differences in the SUVmax (P<0.001) and TNR (P< 0.001) among the four groups (Table 2). As the maximum tu-

Table 1. *Comparison of SUVmax and TNR among groups with different degrees of differentiation.*

Group	SUVmax			TNR		
	median	quartile range	P value	median	quartile range	P value
moderately differentiated (n=45)	7.80	6.40～10.10	0.033	2.56	2.11～3.70	0.044
moderately-poorly differentiated (n=51)	9.60	6.40～12.90		3.17	2.37～4.57	
poorly differentiated (n=20)	11.10	7.83～14.63		3.76	2.99～4.19	

mor diameter increases, SUVmax and TNR gradually increase.

Among the 116 lesions, 38 lesions were classified into the low Ki67 expression group and the remaining 78 lesions were classified into the high Ki67 expression group. There were significant differences in the SUVmax (P=0.028) and TNR (P=0.007) between the two groups. As the Ki67 expression increased, SUVmax and TNR also increased gradually (Table3).

Maximum SUV was significantly correlated with differentiation (r=0.244, P=0.008), tumor size (r=0.481, P<0.001), and Ki67 expression (r=0.242, P=0.009) by Spearman correlation analysis. The poorer the degree of differentiation, the larger the tumor, and the higher the expression of Ki67, the higher the degree of ^{18}F-FDG uptake (Figure 1).

Discussion

In the diagnosis of tumors, ^{18}F-FDG PET mainly uses the degree of uptake of ^{18}F-FDG by tumor cells. Fluorine-18-FDG is a glucose analog that competes with glucose for transporting into cells by the GLUT 1 and 3 transporters. After becoming phosphorylated by hexokinase, ^{18}F-FDG-phosphate cannot undergo glycolysis and is effectively trapped in cells. Thus, PET imaging showed that ^{18}F-FDG uptake is enhanced. Fluorine-18-FDG PET has low detection sensitivity for primary liver cancer lesions, mainly due to the low detection rate of HCC (40–63.1%) [10-12]. Hepatocellular carcinoma can be imaged with ^{18}F-FDG PET owing to the high levels of phosphatase, which dephosphorylates ^{18}F-FDG and allows it to diffuse out of cells. Studies by Iwata et al. (2000) [13] show that ^{18}F-FDG PET/CT has a sensitivity of 92% for patients with ICC, and most of the lesions show high ^{18}F-FDG uptake. The results of this study show that for moderately and poorly differentiated ICC, as the degree of differentiation is worse, the higher the degree of malignancy, the higher the SUVmax and TNR of the tumor cells; further, the SUVmax is significantly related to the degree of tumor cell differentiation, indicating that the degree of ^{18}F-FDG uptake and the malignancy of ICC were positively correlated. The result is similar to related studies showing that the uptake of ^{18}F-FDG is significantly related to the degree of HCC differentiation [14, 15].

There was a significant correlation between the semi-quantitative index of SUVmax and TNR, which may both be able to reflect the characteristics of ICC such as the pathological differentiation and tumor size [8, 16]. This study showed significant differences in the SUVmax and TNR groups among the different groups of maximum tumor diameters. Moreover, SUVmax was significantly related to the maximum tumor diameter. It shows that the uptake of ^{18}F-FDG by large ICC, especially huge ICC, is significantly higher than that of small ICC, and ^{18}F-FDG PET/CT is relatively easier to detect. It is therefore hypothesized that high ^{18}F-FDG uptake directly reflects the level of metabolic activity of a lesion, and a metabolically active lesion will

Table 2. *Comparison of SUVmax and TNR among groups with different tumor size.*

Group	SUVmax			TNR		
	median	quartile range	P value	median	quartile range	P value
⩽3cm（n=14）	6.50	4.70～8.45	<0.001	2.50	1.71～2.93	<0.001
>3cm and ⩽5cm（n=37）	7.70	6.10～10.40		2.53	2.01～3.95	
>5cm and ⩽10cm（n=52）	10.35	8.40～14.55		3.45	2.89～4.43	
>10cm（n=13）	12.10	8.60～13.35		3.90	3.01～5.80	

Table 3. *Comparison of SUVmax and TNR between groups with different Ki67 expression levels*

Group	SUVmax			TNR		
	median	quartile range	P value	median	quartile range	P value
low Ki67 expression (n=38)	7.65	5.08～11.13	0.028	2.45	1.77～3.87	0.007
high Ki67 expression (n=78)	9.30	7.48～12.43		3.29	2.55～4.35	

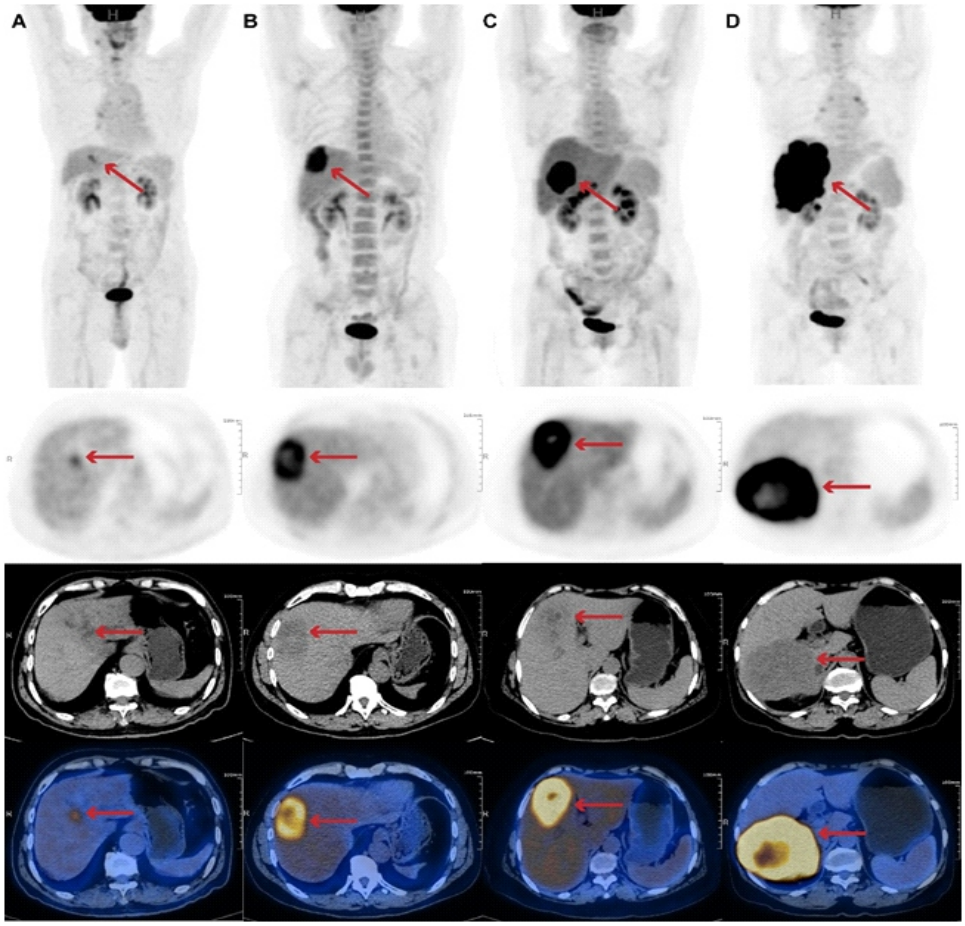

Figure 1. A. A 74-year-old male with moderately differentiated intrahepatic cholangiocarcinoma (ICC) in the left lobe of the liver. The lesion size was about 2.0cm×2.0cm and the corresponding maximum standardized uptake value (SUVmax) was 5.0; B. A 59-year-old man with moderately-poorly differentiated ICC in the right lobe of the liver. The lesion size was 5.0cm×4.0cm and the corresponding SUVmax was 7.7; C. A 53-year-old woman with poorly differentiated ICC in the left lobe of the liver. The lesion size and SUVmax of the lesion were 7.0cm×6.0cm and 14.7, respectively; D. A 61-year-old woman with moderately differentiated ICC in the right lobe of the liver. The lesion size and SUVmax of the lesion were 12.0cm×8.0cm and 31.5.

grow at a faster rate. As already suggested by Ishita et al. [17], such an indication may eventually lead us to consider earlier or more active monitoring and intervention.

As a tumor marker, the Ki-67 antigen has been widely used to determine the level of proliferation of tumor cells in some malignant tumors [18-21]. The Ki-67 antigen encodes two isoform proteins with molecular weights 345kDa and 395kDa initially identified by Scholze and Garden in the early 1980s. This protein appears in all active phases of the cell cycle, namely G1, S, G2, and M, but does not appear in the G0 phase [22, 23]. Ki-67 is at a low level in the G1 and S phases and reaches a peak at the beginning of the mitotic phase, but in the next phase of mitosis, there is a decrease in Ki-67 levels. The expression of Ki-67 that appears in the cell cycle will be governed by the right balance between synthesis and degradation, which is characterized by a short Ki-67 half-life, i.e., 1-1.5h. The Ki-67 expression is associated with the proliferative activity of intrinsic cell populations of malignant tumors; thus, these markers can be used to assess the tumor aggressiveness [24]. The results of this study show that the SUVmax and TNR of the Ki67 high expression group are significantly higher than those of the Ki67 low expression group, and the SUVmax is significantly related to tumor Ki67 expression, further suggesting that the higher the degree of ^{18}F-FDG uptake, the poorer the differentiation degree and the faster the cell proliferation of ICC.

In conclusion, the degree of ^{18}F-FDG uptake in moderately and poorly differentiated ICC is significantly related to tumor size, differentiation, and Ki67 expression. The poorer the degree of differentiation, the larger the tumor, and the higher the expression of Ki67, the higher the degree of ^{18}F-FDG uptake, and the faster the cell proliferation.

Acknowledgement

This study is supported by Science and Technology Committee of Shanghai Municipality (Grant No. 20DZ2201800), the Youth Medical Talents-Medical Imaging Practitioner Program of Shanghai "Rising Stars of Medical Talent" Youth Development Program (SHWRS (2020)_087), Special Fund for Clinical Research of Zhongshan Hospital, Fudan University (2020ZSLC63) and Shanghai Municipal Key Clinical Specialty (shslczdzk03401).

The authors declare that they have no conflicts of interest.

Bibliography

1. Shaib YH, Davila JA, McGlynn K et al. Rising incidence of intrahepatic cholangiocarcinoma in the United States: a true increase? *J Hepatol* 2004; 40:472-7.
2. Lee JD, Kang WJ, Yun M. Primary cancer of the liver and biliary duct. *PET Clin* 2008; 3(2) 169-86.
3. Corvera CU, Blumgart LH, Akhurst T et al. ^{18}F-fluorodeoxyglucose positron emission tomography influences management decisions in patients with biliary cancer. *J Am Coll Surg* 2008; 206: 57-65.
4. Petrowsky H, Wildbrett P, Husarik DB et al. Impact of integrated positron emission tomography and computed tomography on staging and management of gall bladder cancer and cholangiocarcinoma. *J Hepatol* 2006; 45: 43-50.
5. Seo S, Hatano E, Higashi T et al. Fluorine-18 fluorodeoxyglucose positron emission tomography predicts lymph node metastasis, P-glycoprotein expression, and recurrence after resection in mass-forming intrahepatic cholangiocarcinoma. *Surgery* 2008; 143: 769-77.
6. Hwang JP, Moon JH, Kim HK, et al. Prognostic value of metabolic parameters measured by pretreatment dual-time-point ^{18}F-fluorodeoxyglucose positron emission tomography/computed tomography in patients with intrahepatic or perihilar cholangiocarcinoma: A STROBE study. *Medicine (Baltimore)* 2021; 100(21): e26015.
7. Yoh T, Seo S, Morino K et al. Reappraisal of Prognostic Impact of Tumor SUVmax by ^{18}F-FDG-PET/CT in Intrahepatic Cholangiocarcinoma. *World J Surg* 2019; 43(5): 1323-31.
8. Jiang L, Tan H, Panje CM et al. Role of ^{18}F-FDG PET/CT Imaging in Intrahepatic Cholangiocarcinoma. *Clin Nucl Med* 2016; 41(1): 1-7.
9. Cao Y, Ke R, Wang S et al. DNA topoisomerase IIα and Ki67 are prognostic factors in patients with hepatocellular carcinoma. *Oncol Lett* 2017; 13(6): 4109-16.
10. Liu TQ, Fan J, Zhou L et al. Effects of suppressing glucose transporter-1 by an antisense oligodeoxynucleotide on the growth of human hepatocellular carcinoma cells. *Hepatobiliary Pancreat Dis Int* 2011; 10(1): 72-7.
11. Tan CH, Thng CH, Low AS et al. Wash-out of hepatocellular carcinoma: quantitative region of interest analysis on CT. *Ann Acad Med Singapore* 2011; 40(6): 269-75.
12. Wang SB, Wu HB, Wang QS et al. Combined early dynamic ^{18}F-FDG PET/CT and conventional whole-body ^{18}F-FDG PET/CT provide one-stop imaging for detecting hepatocellular carcinoma. *Clin Res Hepatol Gastroenterol* 2015; 39(3): 324-30.
13. Iwata Y, Shiomi S, Sasaki N et al. Clinical usefulness of positron emission tomography with fluorine-18-fluorodeoxyglucose in the diagnosis of liver tumors. *Ann Nucl Med* 2000; 14(2): 121-6.
14. Shin JA, Park JW, An M et al. Diagnostic accuracy of ^{18}F-FDG positron emission tomography for evaluation of hepatocellular carcinoma. *Korean J Hepatol* 2006; 12: 546-52.
15. Lee JD, Yang WI, Park YN et al. Different glucose uptake and glycolytic mechanisms between hepatocellular carcinoma and intrahepatic mass-forming cholangiocarcinoma with increased ^{18}F-FDG uptake. *J Nucl Med* 2005; 46: 1753-9.
16. Kim YJ, Yun M, L WJ et al. Usefulness of ^{18}F-FDG PET in intrahepatic cholangiocarcinoma. *Eur J Nucl Med Mol Imaging* 2003; 30: 1467-72.
17. Singh I, Bikas A, Garcia CA et al. ^{18}F-FDG-PET SUV as a prognostic marker of increasing size in thyroid cancer tumors. *Endocr Pract* 2017; 23(2): 182-9.
18. Gandini S, Guerrieri-Gonzaga A, Pruneri G et al. Association of molecular subtypes with Ki-67 changes in untreated breast cancer patients undergoing pre-surgical trials. *Ann Oncol* 2014; 25: 618-23.
19. Marinescu A, Stepan AE, Mărgăritescu C et al. P53, p16 and Ki67 immunoexpression in cutaneous squamous cell carcinoma and its precursor lesions. *Rom J Morphol Embryol* 2016; 57(2): 691696.
20. Alferraly IT, Munir D, Putra IB. Correlation of Ki-67 Expression as Tumor cell Proliferation Activity Marker with Cutaneous Squamous Cell Carcinoma Grading. *Open Access Maced J Med Sci* 2019; 7: 3384-6.
21. Ahmad B, Asif M, Ali A et al. Expression of Ki-67 and Beta-Catenin in Pseudoepitheliomatous Hyperplasia and Squamous Cell Carcinoma in Oral Mucosal Biopsies: An Immunohistochemical Study. *Asian Pac J Cancer Prev* 2020; 21: 157-61.
22. Geng XF, Fang M, Liu SP, Li Y. Quantum dot-based molecular imaging of cancer cell growth using a clone formation assay. *Mol Med Rep* 2015; 14: 3007-12.
23. Marinescu A, Stepan AE, Mărgăritescu C et al. P53, p16 and Ki67 immunoexpression in cutaneous squamous cell carcinoma and its precursor lesions. *Rom J MorpholEmbryol* 2016; 57(2): 691-6.
24. Li LT, Jiang G, Chen Q, Zheng JN. Ki-67 is a promising molecular target in the diagnosis of cancer (Review). *Mol Med Rep* 2015; 11: 1566-72.